ELSEVIER

Chemical Engineering Journal 131 (2007) 171–179

Chemical Engineering Journal

www.elsevier.com/locate/cej

Distribution optimization for plate-fin catalytic combustion heat exchanger

Sheng Wang, Shudong Wang *

Dalian Institute of Chemical Physics, Chinese Academy of Sciences, Dalian 116023, PR China

Received 24 August 2006; received in revised form 21 December 2006; accepted 21 December 2006

Abstract

The characteristics of a plate-fin catalytic combustion heat exchanger (PFCCHE) which integrates catalytic combustion and heat exchange into one device have been investigated by experiment and numerical simulation. One combustion chamber was integrated with two evaporation chambers to constitute a single unit of PFCCHE. The Pt/Al_2O_3 catalyst pellets were packed into the combustion chamber. The uniform concentration and temperature distribution contributes to the higher thermal efficiency of PFCCHE. A porous media model was supplied to three-dimensional computational fluid dynamics (CFD) simulations of flow field in the PFCCHE. And cold test was performed to validate the numerical model. Results indicated that the numerical prediction of the porous media model was in agreement with experimental data. Fluid maldistribution was observed for the first generation distributor. Thus a second distributor was designed and validated by the cold- and hot-state experiments. Scale-up for 5 kW fuel processing system was performed successfully.

Keywords: Packed bed; Porous media; Distributor; CFD

1. Introduction

Compared with ordinary flame combustion, catalytic combustion has been widely applied due to its unique features. Lower combustion temperature can avoid the thermal NO*x* production, and lower lean limit of flammability can achieve the stable combustion of lean fuels such as fuel cell anode off-gases [1]. These features provide the basis for the development of more efficient, cleaner and safer equipment or process.

The catalytic combustion heat exchanger (CCHE) integrates catalytic combustion and heat exchange into a single device, thus capable of replacing the conventional boiler and heat exchanger. Some improvements were done to intensify heat transfer from the following aspects: the catalyst-loading mode, cross-section structure of CCHE as well as hydraulic diameter of channel when phase change happens. The wall coating catalyst represents a superior geometry due to the lower pressure drop as well as improved heat transfer [2]. Further studies demonstrated that channel dimensions play a critical role in determining heat transfer mechanisms and have a strong effect on the heat transfer coefficient [3]. Compared with finned tube heat exchanger, plate-fin heat exchanger (PFHE) is easier to scale up and can provide larger heat transfer area as well as multi-stream configuration. Due to its large heat transfer area (around 2500 $m^2\ m^{-3}$), compact structure (fins and flat plates with a thickness of 0.2 mm) and high heat transfer coefficient (up to 9697 $W\ m^{-2}$ s), many applications of PFHE have been achieved in such fields such as air separation and petrochemical industries. In this paper, PFCCHE was derived from PFHE.

The nonuniformity of flow field is detrimental to longitudinal wall conduction and the distribution of the interior temperature, which is the main reason that causes the deterioration of heat exchanger efficiency, especially for the compact heat exchanger [4,5]. It has been well recognized that the flow nonuniformity through the exchanger is generally associated with improper exchanger entrance configuration. Therefore, most of previous studies mainly investigated the effects of different header configurations on the fluid flow distribution in PFHEs and tried to minimize the effect of flow maldistribution by optimizing the design of header configuration for PFHEs [4–8], with more attention paid to the optimization of industry-scale exchangers. Their large dimension of optimized distribution methods is not suitable for PFCCHE. So it is impossible to apply the previous improvements on the header configuration of PFHE to the

* Corresponding author. Tel.: +86 411 84662365; fax: +86 411 84662365.
E-mail address: Wangsd@dicp.ac.cn (S. Wang).

1385-8947/$ – see front matter © 2007 Elsevier B.V. All rights reserved.
doi:10.1016/j.cej.2006.12.035

Nomenclature

C, D	the prescribed matrices
C_p	molar capacity ($J\,K^{-1}\,mol^{-1}$)
C_s	species mass fraction
C_2	inert resistant factor (m^{-1})
D_p	mean diameter of catalyst pellets (m)
f_{ave}	the mean molar fraction
f_n	the specie mole fraction in nth sampling location
L	height of packed bed (along the flow direction) (m)
N	the number of concentration collector
Δp	pressure drop in the packed bed (Pa)
S_D	standard deviation
S_i	source items in the ith dimension
v_i	velocity in ith (x, y, z) dimension ($m\,s^{-1}$)
v_j	the velocity components in the x, y, and z directions for differential units ($m\,s^{-1}$)
v_∞	the velocity of a 100% open area ($m\,s^{-1}$)

Greek letters

α	permeability (m^2)
ε	porosity of the packed bed
μ	viscosity ($kg\,m\,s^{-1}$)
ρ	density of fluid ($kg\,m^{-3}$)

optimization of PFCCHE. In PFCCHE, temperature distribution is strongly dependent on concentration distribution. When the fuel with high calorific value is used such as CH_4, CH_3OH and H_2, non-uniformity of concentration distribution will lead to the occurrence of local hot spot, resulting in the deterioration of the thermal efficiency of PFCCHE, which would be a security hazard for operation. So it is necessary to study the concentration distribution in PFCCHE. The realization of uniform distribution will contribute to the enhancement of the heat transfer and thermal efficiency of PFCCHE.

The objective of the present study is to identify the uniformity of the concentration distribution in PFCCHE under different operating conditions and improve its flow flied distribution. First of all, experimental and theoretical researches were performed on cold test concentration distribution in PFCCHE. Then a numerical model predicting the performance of the conventional distributor was proposed and its validity was discussed by comparing experimental and numerical results. Finally, a novel distributor was designed. Its performance was evaluated by cold- and hot-state experimental researches. The distribution behavior of its scale-up was also studied.

2. Experimental

2.1. Plate-fin catalytic combustion heat exchanger

A pilot PFCCHE was designed and installed. The PFCCHE is composed of three chambers. Catalytic combustion reaction occurs in the middle chamber. Evaporation process arises in two symmetrical side ones. Cross flow arrangement was adopted. Some 30–40 mesh combustion catalyst pellets (Pt/Al_2O_3) were packed into the combustion chamber. The catalyst, which was developed independently in our laboratory, has been widely applied in the removal of VOC as a commercial catalyst and exhibited durable stability in long-term stability testing lasting for thousands of hours. During experiment, H_2/air was ignited at ambient temperature over the catalyst. The detailed drawing and photograph of PFCCHE are presented in Fig. 1. According to practical needs, PFCCHE can be expediently scaled up.

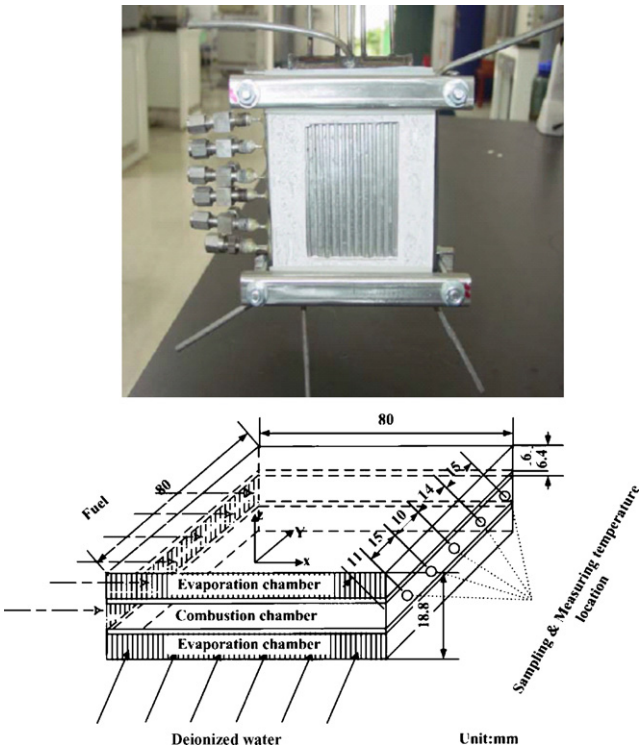

Fig. 1. Photograph and schematic drawing of the catalytic combustion heat exchanger.

2.2. Experimental procedure

Gaseous reactants entered the system at room temperature, and their individual flow rates were regulated by mass flow controller. Different evaporated liquids were supplied into the evaporation chamber by flow pump. A schematic drawing of the experimental system is shown in Fig. 2. Fuel and oxidant passed through their distributors and then entered the combustion chamber of PFCCHE. During experiments, hydrogen and air were used as working medias, and deionized water as evaporated fluid. Methane or other combustible gases were also used as fuels. For the generating hydrogen system fed by liquid fuels such as methanol, ethanol or gasoline, partial anode off-gases from fuel cell returned PFCCHE and supplied heat directly to the endothermic process in evaporation chamber. Then superheated steams were supplied to the reformer. The PFCCHE was made of stainless steel 304, which has a good heat-transfer capability. The center parts of two side plates were caved to embed into two symmetric glass windows. Thus protuberant part of the quartz

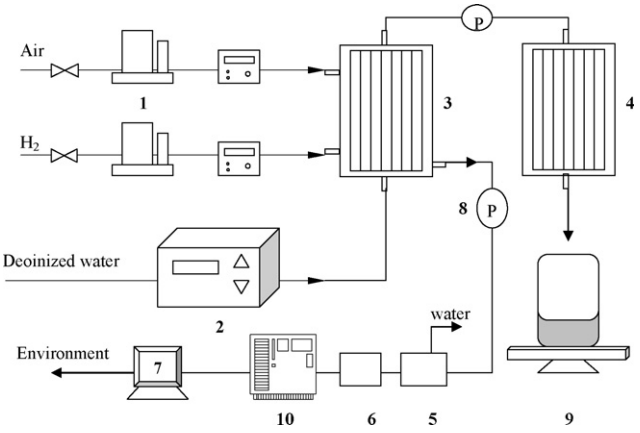

Fig. 2. Schematic diagram of the experimental system. (1) Mass flow controller, (2) pump, (3) catalytic combustion plate-fin heat exchange, (4) condenser, (5) gas–liquid separator, (6) desiccator, (7) PC-control, (8) pressure meter, (9) scale and (10) GC.

glass was just close to the exposed plate-fin. Through the glass window, the boiling behaviors were observed. During experiments, the PFCCHE was placed vertically and insulated well by wrapping quartz cotton. Fuel and oxidant were introduced into the combustion chamber, combusting over the Pt/Al_2O_3 catalyst. In the evaporation chamber, deionized water supplied from the bottom was gasified. Then steam was condensed and scaled to calculate the average heat transfer coefficient. The combustion tail gases were condensed and dried, then analyzed with an on-line gas chromatograph (GC-7890, Techcomp Co., Shanghai, China), using a thermal conductivity detector (TCD), and with helium as carrier gas. The total flow rate of off gases was calculated by a nitrogen balance method. Concentration distribution was also detected by collecting gases in various sampling locations. And temperature distribution was rather determined by thermocouples.

To investigate the initial concentration distribution, air was substituted for nitrogen because of their approximate diffusive coefficients. Then temperature distribution in combustion chamber was studied in the hot-state experiments.

2.3. Distributors

Due to the rather small dimension of the cross section in the combustion chamber, special gas distributors were designed and fabricated. A "comb" structure was used for H_2 distributor and a simple tubular structure was used for air distribution. Their configurations are shown in Fig. 3, with detailed specifications listed in Tables 1–3.

Table 1
Geometrical details of the combustion chamber and numerical domain used

Dimension	mm
Length	80
Width	80
Height	6

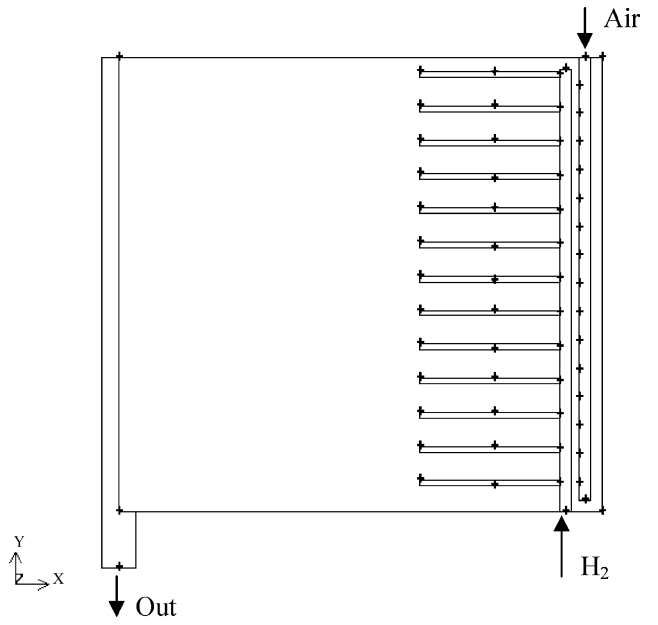

Fig. 3. Sketch of combustion chamber and the computational domain in the catalytic combustion heat exchanger.

3. Numerical simulations

In cold test, no heat transfer occurs. So the governing equations for fluid flow in the combustion chamber are continuity equation, momentum equation and species equations for each species. With more attention paid on steady concentration distribution, no temporal variance is involved in the governing equations.

- Continuity equation:

$$\frac{\partial u}{\partial x} + \frac{\partial \upsilon}{\partial y} + \frac{\partial w}{\partial z} = 0 \tag{1}$$

- Species transport equation:

$$\frac{\partial(uC_s)}{\partial x} + \frac{\partial(\upsilon C_s)}{\partial y} + \frac{\partial(wC_s)}{\partial z} = \frac{\partial}{\partial x}\left(D_s \frac{\partial C_s}{\partial x}\right) + \frac{\partial}{\partial y}\left(D_s \frac{\partial C_s}{\partial y}\right) + \frac{\partial}{\partial z}\left(D_s \frac{\partial C_s}{\partial z}\right) + S_s \tag{2}$$

When no reactions occur in the system, source term in Eq. (2) is equal to 0.

- Momentum equation:

$$\frac{\partial(\rho u u_i)}{\partial x} + \frac{\partial(\rho \upsilon u_i)}{\partial y} + \frac{\partial(\rho w u_i)}{\partial z} = \frac{\partial}{\partial x}\left(\mu \frac{\partial u_i}{\partial x}\right) + \frac{\partial}{\partial y}\left(\mu \frac{\partial u_i}{\partial y}\right) + \frac{\partial}{\partial z}\left(\mu \frac{\partial u_i}{\partial z}\right) - \frac{\partial p}{\partial x_i} + S_i \tag{3}$$

Table 2
Configuration parameters of H_2 distributor

Distributor	Diameter (mm)	Branch			Number of holes in each branch	Hole diameter (mm)
		Number	Length (mm)	Diameter (mm)		
H_2	4	13	27	1	2	0.5

Table 3
The characteristics of the air distributor

Distributor	Air
Diameter (mm)	4
Number of holes	15
Hole diameter (mm)	0.5

For combustion chamber packed with catalyst pellets, porous media model should also be included in the governing equations. Generally porous media are modeled by the addition of a momentum source term to the standard momentum equation [9]. The source term consists of a flow resistance term based on Darcy law (the first term on the right-hand side of Eq. (4)), and an inertial loss term (the second term on the right-hand side of Eq. (4)):

$$S_i = -\sum_{j=1}^{3} D_{ij}\mu v_j + \sum_{j=1}^{3} C_{ij}\frac{1}{2}\rho|v_j|v_j \tag{4}$$

Through simplification, the expression becomes

$$S_i = -\left(\frac{\mu}{\alpha}v_i + C_2\frac{1}{2}\rho|v_i|v_i\right) \tag{5}$$

in which the permeability, α and inertial loss coefficient, C_2 in each component direction are calculated by following expressions:

$$\alpha = \frac{D_p^2}{150}\frac{\varepsilon^3}{(1-\varepsilon)^2} \tag{6}$$

$$C_2 = \frac{3.5}{D_p}\frac{1-\varepsilon}{\varepsilon^3} \tag{7}$$

Due to momentum dissipation, pressure drop will enhance. A semi-empirical correlation is adopted to calculate pressure drop. The formula is appropriate over wide Re range for different packed methods. Its expression is

$$\frac{|\Delta p|}{L} = \frac{150\mu}{D_p^2}\frac{(1-\varepsilon)^2}{\varepsilon^3}v_\infty + \frac{1.75\rho}{D_p}\frac{1-\varepsilon}{\varepsilon^3}v_\infty^2 \tag{8}$$

For the laminar flow in packed bed, the second term on the right-hand of Eq. (8) can be neglected. Thus Blake–Kozeny empirical equation can be gained:

$$\frac{|\Delta p|}{L} = \frac{150\mu}{D_p^2}\frac{(1-\varepsilon)^2}{\varepsilon^3}v_\infty \tag{9}$$

Using above equations, inertial loss coefficient and permeability can be calculated (see Table 4). The porous media is assumed to be isotropic, therefore the inertial loss coefficient and the permeability in three dimensions are regarded to be the same.

Because of no significant difference between the results using various difference discretization schemes [10] in porous media model, the governing equations, Eqs. (1)–(3), are discretized using the default scheme and solved by an iterative method. The commercial computational fluid dynamics package FLUENT™ is used for numerical simulations.

4. Results and discussion

A complete conversion of H_2 over Pt/Al_2O_3 catalyst has been reached when the molar ratio of air to H_2 is 3.75, which was confirmed in the hot-state experiments. So the operation conditions listed in Table 5 were selected. To reappear the initial field distribution in the combustion chamber, cold-state numerical simulations were performed. Fig. 4 shows the predicted hydrogen concentration profiles inside the catalytic chamber under different GHSV. It showed that with increasing of GHSV concentration distribution worsens, and large eddy rise. This is due to a big difference in the velocity magnitude for different branches of the H_2 distributor or holes of air distributor. And the velocity difference will be enhanced by higher GHSV. The presence of excessive N_2 caused an upward swirl. To improve the field distribution, other attempts were performed depending on the numerical simulation. For instance, changing the exit

Table 5
Operating conditions in the cold-state experiments

N_2 flux ($l\,min^{-1}$)	H_2 flux ($l\,min^{-1}$)	GHSV (h^{-1})
0.75	0.2	2300
1.5	0.4	4600
2.25	0.6	7000
3	0.8	9000

Table 4
Specified boundary conditions

	Packed fed specifications			Catalyst material characters		
	ε	α (m^2)	C_2 (m^{-1})	D_p (mm)	ρ ($g\,ml^{-1}$)	C_p ($J\,K^{-1}\,mol^{-1}$)
Constant	0.372	4.9E−10	5.7E+4	0.75	0.955	77.21

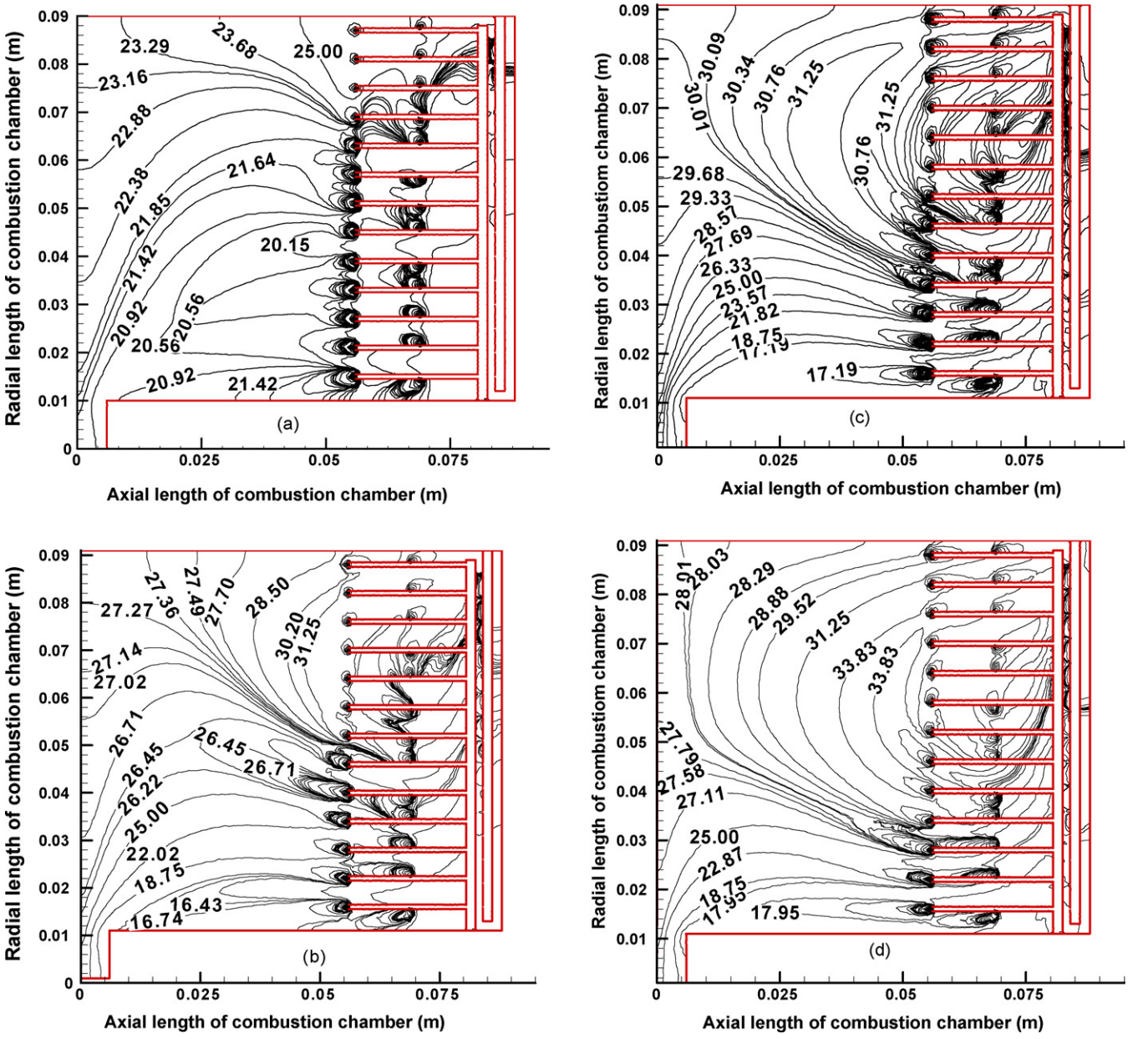

Fig. 4. (a–d) Calculated H_2 concentration profiles in the combustion chamber under different GHSV. (a) GHSV = 2300 h^{-1}, (b) GHSV = 4600 h^{-1}, (c) GHSV = 7000 h^{-1} and (d) GHSV = 9000 h^{-1}.

locations of combustion tail-gases reduced the swirl along the radial coordinate, and adjusting the holes diameters of distributors poised the velocity magnitude through them. But only slight effects were found [11].

Comparisons between the experimental and simulated hydrogen concentration in the combustion chamber were carried out to validate the porous model. The experimental data used in Fig. 5 are the average value of the five trials conducted. Some discrepancy exists between the numerical predictions and experimental measurements. The hydrogen concentration is under-estimated at a certain extent. However, the overall agreement between the numerical and the experimental data is still satisfying. The minor discrepancy may be attributed to the assumptions used in the numerical simulations, which include constant porosity of the packed bed, uniform size of catalyst particles and smooth solid particles [10]. In reality, the porosity is higher near the fin and lower towards the centre of the passage and the particles sizes are not uniform. Also, the shape of the particles is not one-fold and the surface roughness of the particles could increase the momentum dissipation.

5. The development of novel distributor

From above numerical and experimental results, it can be seen that conventional distribution methods cause severe maldistribution in the combustion chamber. To improve the performance of PFCCHE, a new kind of distributor was developed. Tondeur and Luo [12,13] proposed the design and scaling laws of ramified fluid distributors by the constructal approach. The distributor presented below is largely inspired by their work. In the present

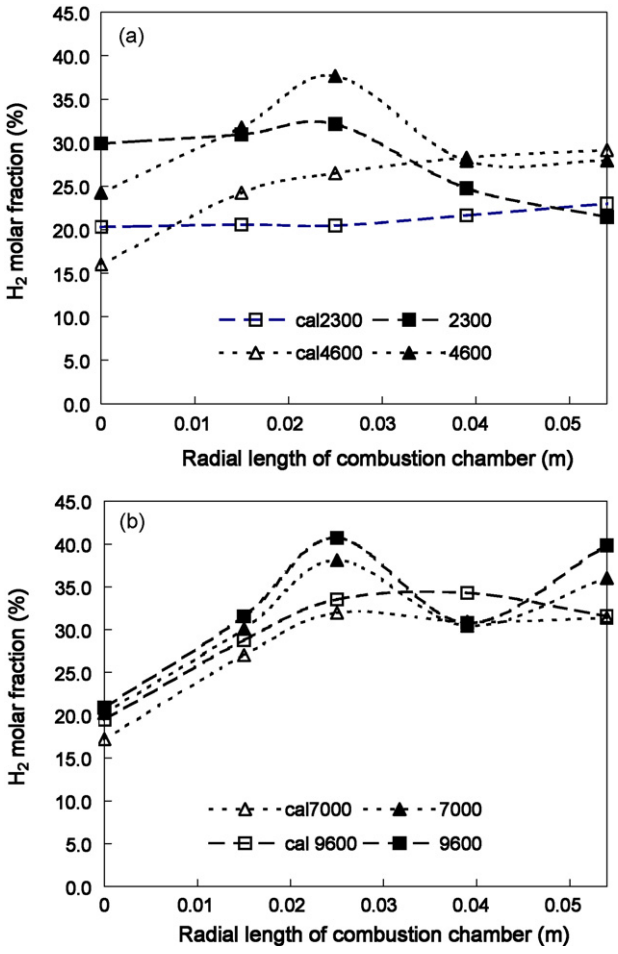

Fig. 5. (a and b) Experimental (solid symbols) and model (hollow symbols) H_2 molar fraction in the combustion chamber as GHSV. (a) Lower GHSV and (b) higher GHSV.

study, a branched fluid distributor was designed and fabricated, as showed in Fig. 6. It has the structure of a sequence of three generations of T- or Y-bifurcations or divisions. Its detailed specifications are displayed in Fig. 6. During experiments, H_2 and N_2 (or air) entered their own distributor with the same structure. To avoid the occurrence of combustion near the inlet of combustion chamber, partial H_2 distribution tubes were inserted into the combustion chamber. Heat transfer module and sampling arrangement remained unchangeable in the CCHE, as shown in Fig. 1.

The distribution characteristics of two distributors were evaluated in the cold-state experiments, as shown in Fig. 7. In theory, uniform field distribution can be established in the combustion chamber for the improved distributor due to its asymmetric structure. The case was also proved by the numerical simulation. So the relevant simulated results were not presented in the paper. From Fig. 7, it can be seen that concentration distribution was improved remarkably for the re-designed distributor, and it keeps similar under various GHSV. In addition, it was found that concentration detected in the sampling point was still deviated from the average values. It is caused by the discrepancy between the assumptions and experiments.

A statistical concept (S_D) was introduced into this paper to evaluate the maldistribution. It is defined as follows:

$$S_D = \sqrt{\frac{1}{N-1}\sum_{n=1}^{N}(f_n - f_{ave})^2} \tag{10}$$

It discloses the dispersion degree of experimental results and reflects the flow maldistribution under different operational parameters.

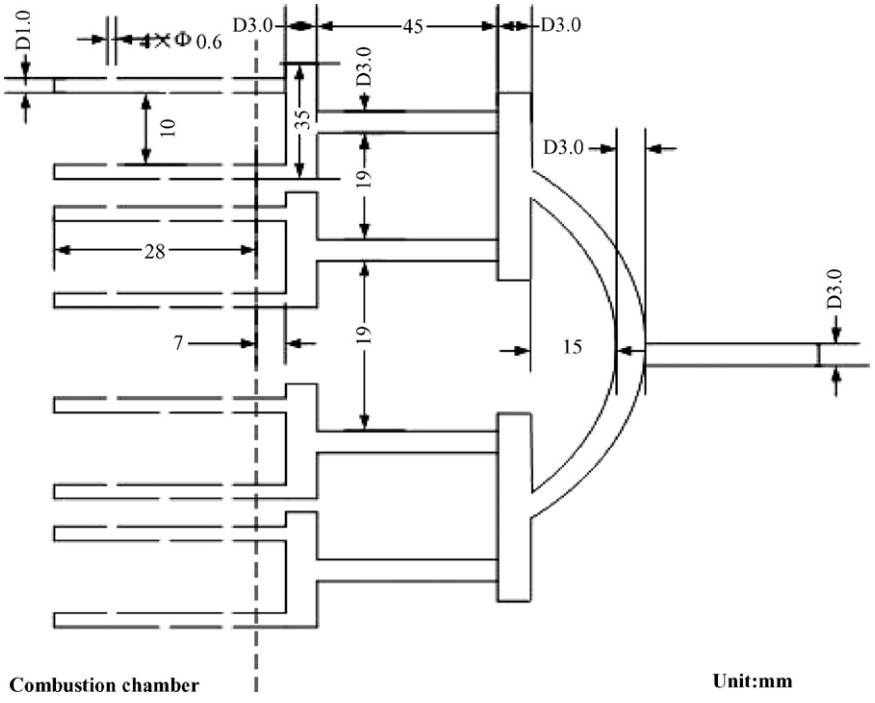

Fig. 6. Sketch of the improved distributor in the combustion chamber of catalytic combustion heat exchanger.

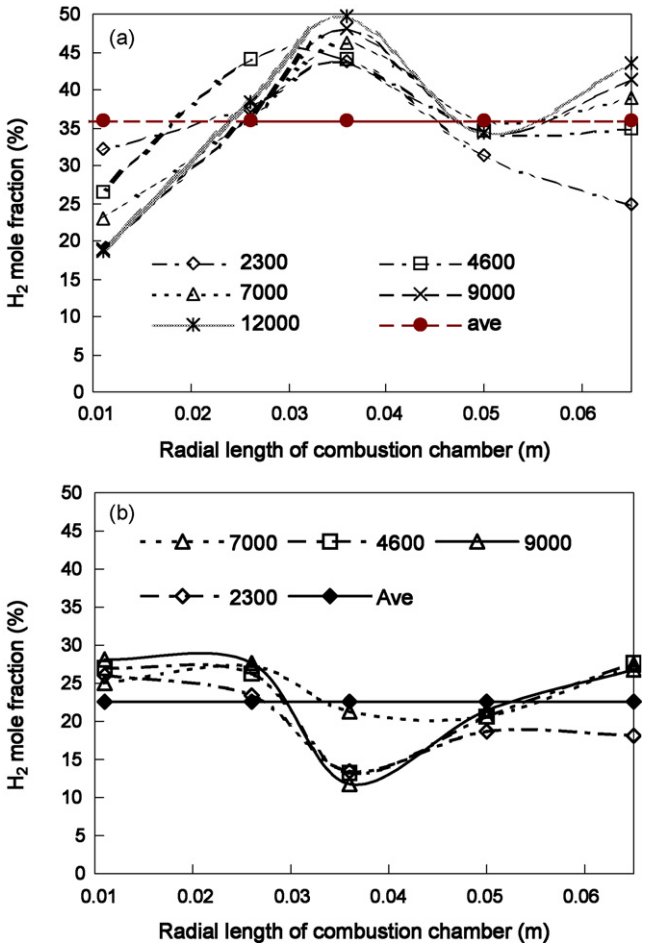

Fig. 7. (a and b) The comparison of distribution effects under different GHSV. (a) The conventional distributor and (b) the improved distributor.

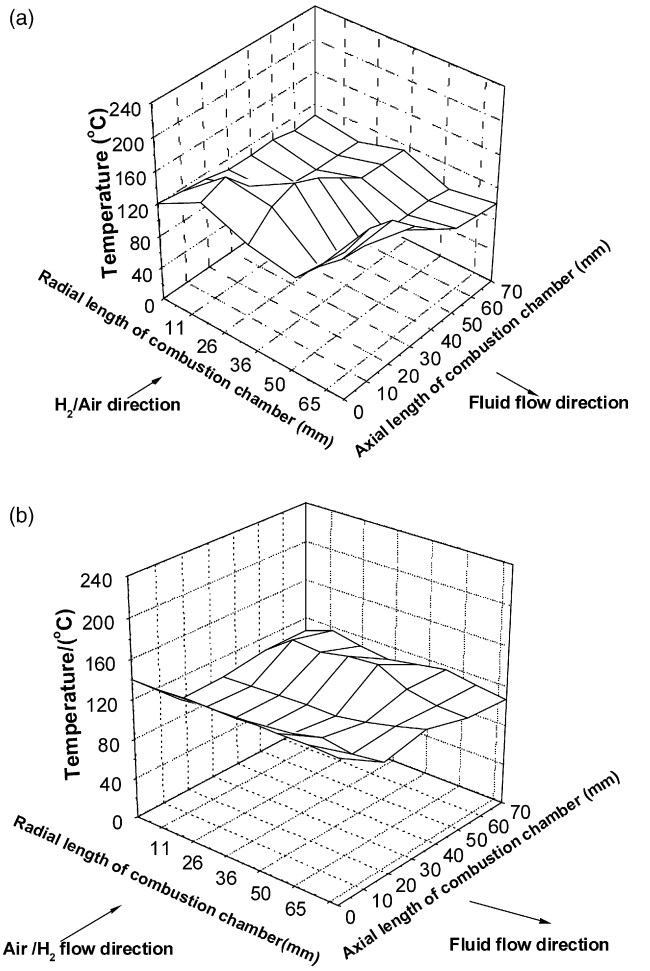

Fig. 8. (a and b) The spatial temperature contours of combustion chamber for different distributors at GHSV = 7000 h^{-1} and deoinized water rate is 3.1 ml min^{-1}. (a) The conventional distributor and (b) the improved distributor.

The maldistribution parameters (S_D) in two kinds of distributors were calculated under different GHSV (see Table 6). Results show that significant maldistribution occurred for the conventional distributor, and the increase of GHSV further deteriorated the flow flied distribution. On the other hand, the behavior of improved distributor kept excellent under various GHSV.

To validate the hot-state distribution effects, their distribution behavior was measured and compared. Under constant operation conditions, spatial temperature contours of two distributors in the combustion chamber are shown in Fig. 8. It can be seen that spatial temperature distribution was relatively even and temperature window existed between 100 and 140 °C for the improved distributor. However local hot-spot (about 180 °C) occurred in the scraggy temperature field for the conventional distributor, and coalesced bubbles only came into being inside these local superheat zones. But uniform nucleated boiling happened in the evaporation chamber for the improved distributor. When the fluid flow rate was the specific value (3.1 ml min^{-1}) referred in Fig. 8, the liquid was completely gasified, and the quantity of evaporation kept constant for the improved distributor. But the amount of evaporation fluctuated around the mean value of 2.9 ml min^{-1} due to the instability of boiling. And the liquid level increased gradually in the evaporation chamber because of the accumulation of partial un-gasified liquid for the conventional distributor. In addition, good distribution characteristics were also validated under other operation conditions [14].

Due to the excellent behavior for improved distributor, scaling up and subsequent application were successfully achieved in a 5 kW fuel processing system. In Fig. 9, a typical PFCCHE

Table 6
Comparisons of distribution behaviors for two distributors

S (%)	GHSV (h^{-1})				
	2300	4600	7000	9000	12000
Conventional distributor	7.14	7.37	8.40	10.91	11.74
Improved distributor	4.92	6.13	3.22	6.9	

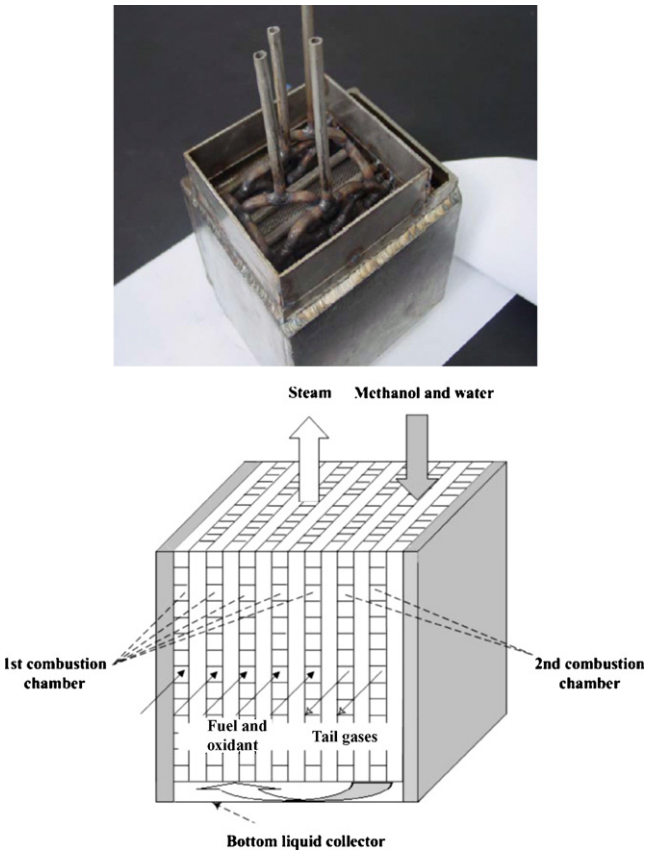

Fig. 9. Photograph and schematic configuration of the PFCCHE in 5 kW fuel processing system.

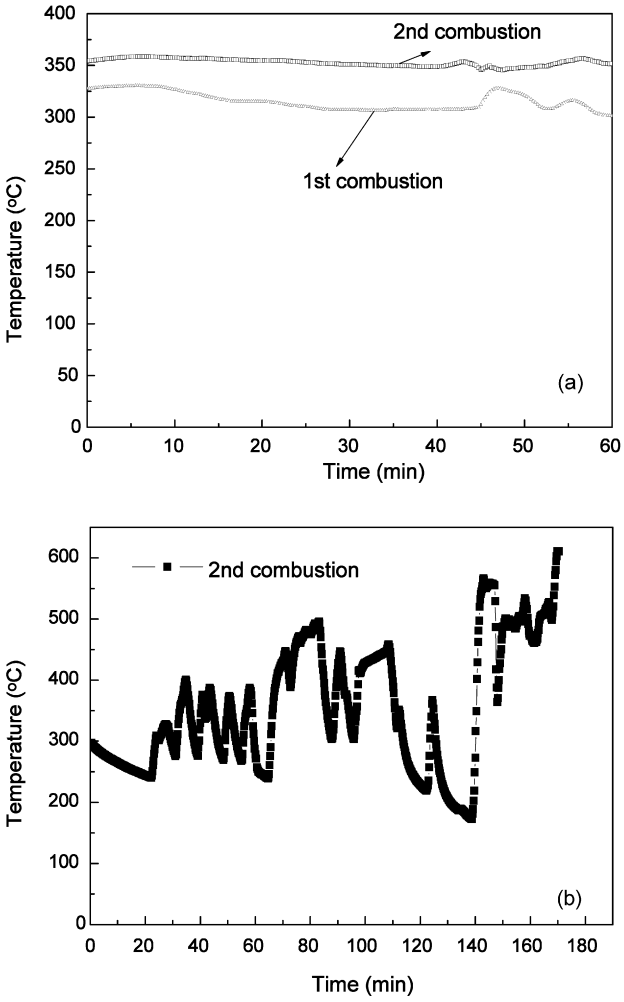

Fig. 10. Performance of (a) improved and (b) first generation distributor system in the scaled up 5 kW size.

applied in a 5 kW fuel processing system is shown. Fuel and oxidant were supplied into the combustion chamber by their own distributor, respectively. Majority of fuel was converted in the first combustion chamber. Then residual fuel was consumed in the second combustion chamber. Methanol and water were preheated in the evaporation chamber adjacent to second combustion chamber, and the heat generated in the first combustion chamber was used to gasify and superheat the preheated methanol and water. Then superheated steam mixture entered the reformer and reacted with air over monolith catalyst. The tail gases from the second combustion chamber were collected in the coiled tubes not shown in Fig. 9. The coiled tubes were placed in the bottom liquid collector and immerged into the evaporated liquid mixture collected. Thus heat was recycled, and the exit temperature of off-gases was decreased to around 130 °C.

Fig. 10 shows the comparison of the application effects for two distribution methods in the 5 kW fuel processing system. It can be seen that the temperature in the first and second combustion chamber kept constant for the improved distributor. And the second combustion temperature is higher than first one. That is due to limited heat transfer area in the evaporation chamber adjacent to second combustion chamber. It is avoided the occurrence of maldistibution in the evaporation chamber adjacent to first combustion chamber, which is caused by partial evaporation of liquid during preheating. This good distribution behavior can ensure the safe and stable operation of PFCCHE. But the rather large temperature fluctuation causes severe instability of the system for the conventional distributor. In addition, improved distributor owns wider operational flexibility, even for the case where pure oxygen was used as oxidant.

6. Conclusions

A highly compact PFCCHE, which is a PFHE-derived integration of catalytic combustion with evaporation, has been explored to substitute for conventional boiler and heat exchanger. Compared with tube-fin configuration, plate-fin structure was adopted to reduce the heat resistance. The PFCCHE is easier to scale up and integrate multi-reaction and heat transfer into a compact device. Uniform concentration and temperature distribution favor the further enhancement the thermal efficiency of PFCCHE. A porous media model was applied in the numerical simulations of flow field in the PFCCHE. Simulation results agreed well with the real spatial concentration distribution. At the same time, results showed that severe maldistribution was significant under various GHSV for the conventional distributor. So the distribution methods were improved based on the constructal theorem. Its good distribution behavior was con-

firmed by the cold- and hot-state experiments. Furthermore its scale-up was designed and applied successfully in a 5 kW fuel processing system. Even though the oxidant is pure oxygen, this kind of distributor exhibited good operational flexibility, thus ensuring the safe and stable operation of the fuel processing system. In addition, the PECCHE can also be used as the domestic boiler or evaporator in the homogenous reaction system in which liquid reactants participate.

Acknowledgements

The authors are grateful to Prof. Xuguang-Liu of Taiyuan University of Technology for his helpful discussion and good advice. This work was financially supported by the National Natural Science Foundation of China (Nos. 20476103 and 20590365). We also gratefully acknowledge the help of Associate Prof. Zhongshan Yuan for supplying the combustion catalysts. Special thanks are offered to the reviewers for their good advice.

References

[1] S. Yong-Seog, Y. Sang-Pil, C. Sung-June, S. Kwang-Sup, The catalytic heat exchanger using catalytic fin tubes, Chem. Eng. Sci. 58 (2003) 43–53.
[2] A. Karim, J. Bravo, A. Datye, Nonisothermality in packed bed reactors for steam reforming of methanol, Appl. Catal. A: Gen. 282 (2005) 101–109.
[3] W. Barbara, Review of saturated flow boiling in small passages of compact heat-exchangers, Int. J. Therm. Sci. 42 (2003) 107–140.
[4] J. Wen, Y. Li, A. Zhou, Y. Ma, PIV investigations of flow patterns in the entrance configuration of plate-fin heat exchanger, Chin. J. Chem. Eng. 14 (2006) 15–23.
[5] W. Jian, L. Yanzhong, Z. Aimin, et al., PIV experimental investigation of entrance configuration on flow maldistribution in plate-fin heat exchanger, Cryogenics 46 (2006) 37–48.
[6] W. Jian, L. Yanzhong, Study of flow distribution and its improvement on the header of plate-fin heat exchanger, Cryogenics 44 (2004) 823–831.
[7] Z. Zhe, L. Yanzhong, CFD simulation on inlet configuration of plate-fin heat exchangers, Cryogenics 43 (2003) 673–678.
[8] J. Anjun, Z. Rui, J. Sangkwon, Experimental investigation of header configuration on flow maldistribution in plate-fin heat exchanger, Appl. Therm. Eng. 23 (2003) 1235–1246.
[9] Fluent 6 User's Guide, Fluent Incorporated Limited, 2001.
[10] S. Natarajan, C. Zhang, T.C. Briens, Numerical simulation and experimental verification of gas flow through packed beds, Powder Technol. 152 (2005) 31–40.
[11] W. Sheng, W. Shudong, Concentration distribution in catalytic combustion heat exchanger at cold state, J. Chem. Indus. Eng. 57 (2006) 558–563 (in Chinese).
[12] L. Luo, D. Tondeur, Optimal distribution of viscous dissipation in a multi-scale branched fluid distributor, Int. J. Therm. Sci. (2005) 1131–1141.
[13] D. Tondeur, L. Luo, Design and scaling laws of ramified fluid distributors by the constructal approach, Chem. Eng. Sci. 59 (2004) 1799–1813.
[14] W. Sheng, Optimization on the key processes of methanol autothermal reforming system for PEMFC, PhD Thesis, Dalian Institute of Chemical Physics, Chinese Academy of Sciences, Dalian, China, 2006.